Shh pathway activation is present and required within the vertebrate limb bud apical ectodermal ridge for normal autopod patterning

Cortney M. Bouldin[a], Amel Gritli-Linde[b], Sohyun Ahn[c], and Brian D. Harfe[a,1]

[a]Department of Molecular Genetics and Microbiology, The Genetics Institute, University of Florida, Gainesville, FL 32610; [b]Department of Oral Biochemistry, Sahlgrenska Academy, University of Gothenburg, Medicinaregatan 12F, SE-41390, Göteborg, Sweden; and [c]Program in Genomics of Differentiation, Eunice Kennedy Shriver-National Institute of Child Health and Human Development, National Institutes of Health, Bethesda, MD 20892

Edited* by Clifford J. Tabin, Harvard Medical School, Boston, MA, and approved February 16, 2010 (received for review November 9, 2009)

Expression of Sonic Hedgehog (*Shh*) in the posterior mesenchyme of the developing limb bud regulates patterning and growth of the developing limb by activation of the Hedgehog (Hh) signaling pathway. Through the analysis of *Shh* and Hh signaling target genes, it has been shown that activation in the limb bud mesoderm is required for normal limb development to occur. In contrast, it has been stated that Hh signaling in the limb bud ectoderm cannot occur because components of the Hh signaling pathway and Hh target genes have not been found in this tissue. However, recent array-based data identified both the components necessary to activate the Hh signaling pathway and targets of this pathway in the limb bud ectoderm. Using immunohistochemistry and various methods of detection for targets of Hh signaling, we found that SHH protein and targets of Hh signaling are present in the limb bud ectoderm including the apex of the bud. To directly test whether ectodermal Hh signaling was required for normal limb patterning, we removed *Smo*, an essential component of the Hh signaling pathway, from the apical ectodermal ridge (AER). Loss of functional Hh signaling in the AER resulted in disruption of the normal digit pattern and formation of additional postaxial cartilaginous condensations. These data indicate that contrary to previous accounts, the Hh signaling pathway is present and required in the developing limb AER for normal autopod development.

limb patterning | polydactyly | Shh signaling

Within the developing limb bud, exposure to SHH controls the number and identity of digits produced. Proper digit patterning requires both the establishment of a concentration-dependent gradient of SHH (1) and a time-dependent gradient of exposure to SHH (2, 3). The ability of SHH to pattern the forming digits is coupled to the ability of SHH to control cell proliferation (4, 5). A full complement of digits requires tight control over the concentration and timing of *Shh* expression. Although SHH is capable of limiting its own expression (6), the molecular mechanism responsible for sensing the amount of SHH from the zone of polarizing activity (ZPA) of the vertebrate limb bud remains unknown.

Through both short-range and long-range signaling (7), secretion of SHH protein from *Shh*-producing cells activates a cellular signal transduction pathway. Binding of SHH protein to the transmembrane protein PTCH1 activates the Hh signaling pathway (8). Once SHH binds to PTCH1, inhibition of another transmembrane bound protein, SMO, is relieved (9). Through a complex of proteins, SMO blocks proteolytic cleavage of members of the Ci/Gli family of transcription factors (10). Uncleaved GLI transcription factors directly activate transcription of hedgehog target genes, such as *Gli1* and *Ptch1* (11, 12).

Within the limb, SHH is involved in a network of positive gene interactions known as the *Shh*/*Grem1*/*Fgf* feedback loop. SHH is capable of up-regulating *Fgf4* expression in the apical ectodermal ridge (AER) (13). Conversely, changes in FGF4 can up-regulate *Shh* expression (14). The Bmp antagonist, *Grem1,* is an intermediate for the interactions between *Shh* and *Fgf4* (15, 16). Regulation of the *Shh*/*Grem1*/*Fgf* feedback loop is essential for proper patterning of the limb and robust regulation of the genes involved in the loop are mediated by regulation of *Grem1* and *Bmp4* (17). Spatial disruption of the positive interactions of the *Shh*/*Grem1*/*Fgf* feedback loop has been shown to terminate feedback loop gene expression (18, 19). In addition to mutual positive interactions within the *Shh*/*Grem1*/*Fgf* feedback loop, the *Etv4*/*5* genes, which are targets of Fgf signaling, are required for proper spatial restriction of *Shh* in the limb bud mesenchyme (20, 21).

Although coordinated regulation of limb development by interactions between the ZPA and AER have been documented (22), the role Hh signaling may play within the limb bud ectoderm is unknown. Previous reports have stated that components required for Hh signaling are not found in the ectoderm of the vertebrate limb bud (23, 24). Recently, treatment of limb buds with the teratogen acetazolamide has uncovered a potential role for Hh signaling in the limb ectoderm. In utero exposure to acetazolamide resulted in limbs with ectrodactyly, phenotypically similar to limbs mutant for *Shh*. However, *Shh* expression in treated limbs was not substantially different from control limbs, suggesting that loss of digits in these animals resulted from defects in the ability of the cells to respond to SHH (25). A series of grafting experiments suggested that the limb bud ectoderm and not the mesoderm was defective in Hh signaling after acetazolamide treatment (25). Microarray experiments in which components of the Hh signaling pathway, but not *Shh*, were identified in the limb bud ectoderm provided further evidence that the Hh signaling pathway may be present in the limb bud ectoderm (26).

In this report, we demonstrate that SHH protein is present and the Hh signaling pathway is required within the limb bud ectoderm for normal autopod patterning to occur. Removal of *Smo*, an essential component of Hh signal transduction, resulted in the disruption of normal digit patterning and formation of additional cartilaginous condensations. Through analysis of mice that lacked Hh signal transduction in the AER and overexpression experiments using the chick model system, we show that the length of the AER is regulated by the Hh signaling pathway. Additionally, Hh signaling within the AER is necessary to refine the expression of genes involved in the *Shh*/*Grem1*/*Fgf* feedback loop. These results uncover a unique role for Hh signal transduction within the vertebrate limb ectoderm and provide

DEVELOPMENTAL BIOLOGY

Author contributions: C.M.B. and B.D.H. designed research; C.M.B., A.G.-L., and S.A. performed research; C.M.B., A.G.-L., S.A., and B.D.H. analyzed data; and C.M.B. and B.D.H. wrote the paper.

The authors declare no conflict of interest.

*This Direct Submission article had a prearranged editor.

[1]To whom correspondence should be addressed. E-mail: bharfe@mgm.ufl.edu.

This article contains supporting information online at www.pnas.org/cgi/content/full/0912818107/DCSupplemental.

further insight into the molecular mechanism responsible for coordinating interactions between the ZPA and AER.

Results

SHH Protein and Components of the Hedgehog Signaling Pathway Are Present in the AER. The secreted protein SHH is produced in mesenchymal cells of the limb bud ZPA (27). Once produced, SHH can spread many cell diameters from its source (7). For the Hh signaling pathway to be active in the ectoderm of the developing limb, SHH protein should be present in this tissue. To investigate SHH protein localization in the limb bud ectoderm, immunohistochemistry using an antibody raised against SHH was performed. In the posterior of an embryonic day (E)10.5 limb bud, SHH immunostaining was observed in both the posterior mesoderm and the posterior ectoderm, including the AER (Fig. 1 *A* and *B*) (28). SHH immunostaining was not present in the anterior mesoderm or ectoderm (Fig. 1*C*).

The two additional Hh homologs present in vertebrates, *Dhh* and *Ihh*, are not expressed concomitant with *Shh* in the limb bud (29). To confirm that the staining observed was specific for SHH protein, a section from a limb bud that lacked SHH ($Shh^{\Delta/\Delta}$) was analyzed in a manner identical to the wild-type limb buds and was found to lack immunostaining in both the mesoderm and the ectoderm (Fig. 1*D*). Sections through different regions of the embryo and limb bud confirmed immunoreactivity of SHH in the AER and the specificity of the immunostaining to regions of the embryo known to express SHH (Fig. S1).

If Hh signaling is active within a given tissue, transcriptional targets of this pathway should be present. Active Hh signaling transcriptionally activates expression of *Gli1* (30). Using a tamoxifen-inducible *Gli1-CreER*^{T2} allele (2) in combination with the cre-inducible *R26R* allele (31), we fate mapped cells that activate the *Gli1* promoter in the mouse limb. Administration of tamoxifen at E9.5 resulted in detection of β-galactosidase activity in the ectoderm of the autopod and zeugopod in embryos at E12.5 (Fig. S1; ref. 32). To confirm that Hh signaling is present in the limb bud ectoderm, we analyzed another Hh pathway target gene, *Ptch1* (33). Mice with a *LacZ* cassette inserted downstream of the endogenous *Ptch1* promoter produce β-galactosidase activity in cells that have activated transcription from the *Ptch1* locus (34). In limbs containing the *Ptch1:LacZ* allele, β-galactosidase activity was detected at E11.5 in the posterior limb bud ectoderm, including the posterior AER (Fig. 1 *E* and *F*). Further analysis revealed that β-galactosidase activity initially appeared punctate in the posterior of the limb, including the ectoderm at E10.0 with robust expression in the ectoderm observed beginning at E10.5 and continuing through E12.5 (Fig. S2). Sectioned limbs contained β-galactosidase activity in both the posterior mesoderm and ectoderm (Fig. 1*G*). Examination of sections revealed detectable β-galactosidase activity in the posterior AER, the posterior dorsal and ventral ectoderm, and the ectoderm of the posterior margin (ectoderm from the posterior AER to the flank; Fig. 1*G* and Fig. S2). These data indicate that SHH is present and capable of activating the Hh signaling cascade within the limb bud ectoderm.

Hedgehog Signaling in the AER Is Required for Formation of a Normal Autopod. Although Hh signal transduction was found in several regions of the ectoderm, because of the importance of the AER in limb development, we chose to focus specifically on activation of the Hh signaling pathway in the AER. SMO, a transmembrane protein required for active Hh signaling (35), was detected in the limb bud ectoderm at E11.5 (Fig. S3). The *Msx2-Cre* allele expresses cre recombinase in the AER but not in the limb mesoderm (Fig. S4) (36). To determine whether Hh signaling in the AER played a functional role in limb patterning, we removed *Smo* from the AER by using *Msx2-Cre* and a conditional allele for *Smo* (see *Methods* for details). Loss of Hh signaling in the ectoderm of

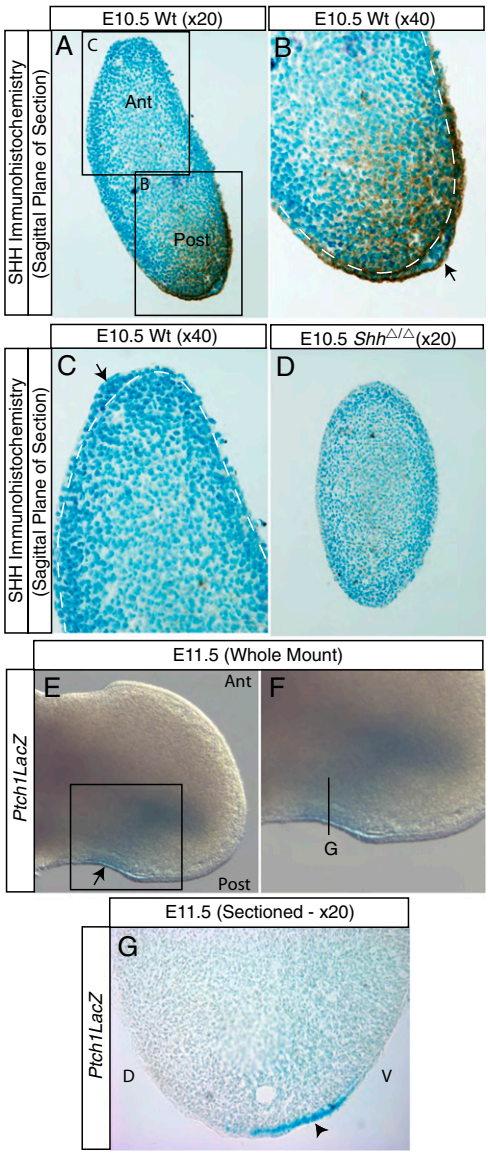

Fig. 1. SHH and components of the hedgehog signaling pathway are present in the limb bud ectoderm. SHH immunohistochemistry on sections from E10.5 forelimbs (*A–D*). (*A*) At low magnification, SHH is detected in a graded fashion specifically in the posterior of the limb. The boxes in *A* are enlarged in *B* and *C*. At high magnification, SHH was visible in the posterior limb bud ectoderm including the AER (*B*), but not the anterior limb bud ectoderm (*C*). In *B* and *C*, the arrows highlight the AER, and the white dashed lines separate the mesoderm from the ectoderm. Limb bud tissue from a $Shh^{\Delta/\Delta}$ limb, which was mounted on the same slide as the tissue shown in *A–C*, had no detectable SHH (*D*). (*E–G*) β-galactosidase activity in limbs containing the *Ptch1:LacZ* allele. (*E*) Whole-mount hindlimbs at E11.5 showed active Hh signaling in the posterior limb mesoderm and ectoderm including the AER. The box in *E* is enlarged in *F*. Sectioned hindlimbs confirmed the presence of β-galactosidase activity in the posterior ectoderm (*G*; arrowhead denotes staining in the ectoderm). The plane of section of *G* is illustrated by a black line in *F*.

embryos in which *Smo* was removed from the AER was confirmed by performing *Ptch1* in situ hybridizations using BM purple as a substrate (*Methods*). Whole-mount RNA in situ hybridizations to detect *Ptch1* at E11.5 revealed expression in the posterior AER of control limbs but not in the AER of *Msx2-Cre;Smo*$^{flox/flox}$ limbs at the same somite stage (ss) (Fig. 2 *A–D*). Sectioned tissue revealed that in *Msx2-Cre;Smo*$^{flox/flox}$ limbs at E10.5 (Fig. S5) and E11.5 (Fig. 2 *E* and *F*) *Ptch1* mRNA was absent from the AER and ventral ectoderm. *Ptch1* was still expressed in the dorsal ectoderm

in addition to the ectoderm proximal to the AER. In situ hybridization with *Ptch1* riboprobe indicated that embryos that had the genotype *Msx2-Cre;Smo*$^{flox/flox}$ have lost Hh signaling from the AER.

To determine whether Hh signaling within the AER played a functional role in the establishment of a proper limb pattern, *Msx2-Cre;Smo*$^{flox/flox}$ and wild-type skeletons were examined. Skeletal analysis revealed that the stylopodal and zeugopodal elements of both *Msx2-Cre;Smo*$^{flox/flox}$ and control limbs were normal (Fig. S5). However, the autopods of the hindlimbs and forelimbs of *Msx2-Cre;Smo*$^{flox/flox}$ animals exhibited extra cartilaginous condensations (Fig. 2 *G–J*), which were highly penetrant (Table S1). Extra cartilaginous condensations were investigated using both *Sox9* expression and bright field microscopy, and were found to be formed between E13.5 and E16.5 (Fig. S6). These data indicate that Hh signaling within the AER is necessary for the formation of a properly patterned autopod. *Msx2-Cre;Smo*$^{flox/flox}$ mice die at birth, which limited our ability to perform a detailed analysis of the extra condensations.

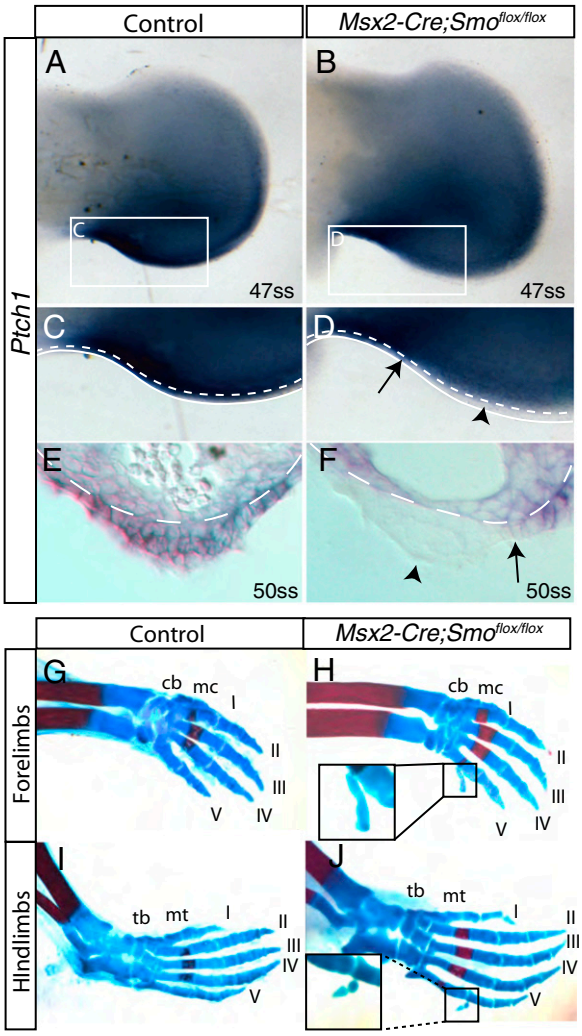

Fig. 2. Hedgehog signal transduction in the AER has a functional role in limb patterning. (*A–F*) RNA in situ hybridizations with control and *Msx2-Cre;Smo*$^{flox/flox}$ limbs by using a riboprobe for *Ptch1*. (*A*) *Ptch1* was expressed throughout the posterior of the control limb at 47ss including the ectoderm. *C* is an enlarged view of the boxed region in *A*. (*B*) In *Msx2-Cre;Smo*$^{flox/flox}$ limbs at 47ss, *Ptch1* is expressed in the posterior limb bud mesoderm and in the most proximal region of the posterior ectoderm, but is not expressed in the AER. *D* is an enlarged view of the boxed region in *B* (arrowhead denotes loss of expression in the AER, whereas the arrow marks expression in the ectoderm adjacent to the AER). Sectioned limbs revealed that *Ptch1* was absent from the AER of *Msx2-Cre;Smo*$^{flox/flox}$ limbs (*F*; arrowhead denotes loss of expression in the AER, whereas the arrow marks expression in ectoderm adjacent to the AER) but present in all posterior ectoderm of the control limbs (*E*). (*C–F*) The white dashed lines highlight the visible boundaries of the mesoderm and ectoderm. (*C* and *D*) The solid white lines highlight the posterior edge of the limb. (*G–J*) Skeletal analysis of P0 limbs. Autopods of *Msx2-Cre;Smo*$^{flox/flox}$ animals exhibited extra cartilaginous condensations in both the forelimbs and hindlimbs (*H* and *J*; see text and Table S1 for details) when compared with controls (*G* and *I*). *H* and *Insets* show the supernumerary cartilaginous condensations found in *Msx2-Cre;Smo*$^{flox/flox}$ animals. cb, carpal bones; mc, metacarpals; tb, tarsal bones; mt, metatarsals.

AER Length Is Controlled by Hh Signaling Within the AER. Signals from the ZPA have been postulated to control the length and shape of the AER (37, 38). *Fgf8* is expressed throughout the entire AER and can be used to measure the length of this structure (Fig. S7) (39, 40). To investigate whether Hh signaling within the limb bud ectoderm regulated the length of the AER, *Fgf8* expression was examined and compared in *Msx2-Cre;Smo*$^{flox/flox}$ and control limbs (Fig. S7). The Straighten plug-in for NIH ImageJ was used to convert the curved AER into a straight-line, which was then measured (*Methods*). Somite matched *Msx2-Cre;Smo*$^{flox/flox}$ forelimbs (50ss; $n = 9$) and hindlimbs (50ss; $n = 10$), and control forelimbs (50ss; $n = 4$) and hindlimbs (50ss; $n = 7$) were collected and analyzed for *Fgf8* expression (for examples, see Fig. S7). Stained AERs were then straightened and measured. AERs in which Hh signaling was removed were found to be on average 700 microns (forelimbs) and 260 microns (hindlimbs) longer than normal limbs at the same somite stage (Fig. 3*A*). The means were compared using a *t* test (Welch's, unpaired), which revealed the increase in AER length in the *Msx2-Cre;Smo*$^{flox/flox}$ limbs to be statistically significant (forelimbs, $P = 0.03$ and hindlimbs, $P < 0.0001$).

Our experiments using the mouse model system indicated that loss of Hh signaling from the AER resulted in an increase in AER length. Using the chick model system, we investigated the effects of elevated amounts of Hh protein on AER length. A SHH-soaked bead placed just anterior to the normal ZPA was used to expand the domain of SHH protein (Fig. 3*B*). After 24 h of treatment with a SHH-soaked bead, the domain of *Ptch1* expression was expanded in the posterior AER (Fig. S8). Limbs treated for 24 h with a SHH-soaked bead also showed a decrease in AER length when compared with the untreated contralateral limb buds or PBS-treated limb buds as measured by *Fgf8* expression (three of four treated limbs; Fig. 3 *C–F*) and *Fgf4* expression (Fig. S9). Consistent with published reports (6), placement of a SHH-soaked bead in the posterior limb bud mesenchyme resulted in an increase in cell death in both the AER and the mesoderm of the limb bud (Fig. S10) but did not cause defects in the patterning of limb skeletal elements, indicating that the limb bud recovers from transient exposure to elevated levels of SHH.

Hedgehog Signaling in the AER Regulates the *Shh/Grem1/Fgf* Feedback Loop. The expression of the genes involved in the *Shh/Grem1/Fgf* feedback loop is dynamic and dependent on the timing and levels of other components in the regulatory network (16–19). To investigate the effect of removal of Hh signaling from the AER on the components of the *Shh/Grem1/Fgf* feedback loop, double RNA in situ hybridizations for *Shh* and *Fgf4* or *Fgf8* were performed on normal and *Msx2-Cre;Smo*$^{flox/flox}$ embryos. *Fgf4* expression was elevated in *Msx2-Cre;Smo*$^{flox/flox}$ limbs compared with wild-type limbs (Fig. 4 *A* and *B*). Additionally, expression of *Fgf8*, which interacts with *Fgf4* (41), was prolonged in *Msx2-Cre;Smo*$^{flox/flox}$ limbs (Fig. 4 *C* and *D*).

Consistent with a link between Fgfs and the expression of *Shh* (41, 42), loss of Hh signaling in the AER resulted in increased expression of *Shh* in the underlying mesenchyme for longer amounts of time than in somite-matched control limbs (Fig. 4 *A* and *B* and Fig. S7). Additionally, analysis of *Msx2-Cre;Smo*$^{flox/flox}$ limbs for *Grem1* expression revealed that the domain of expression

DEVELOPMENTAL BIOLOGY

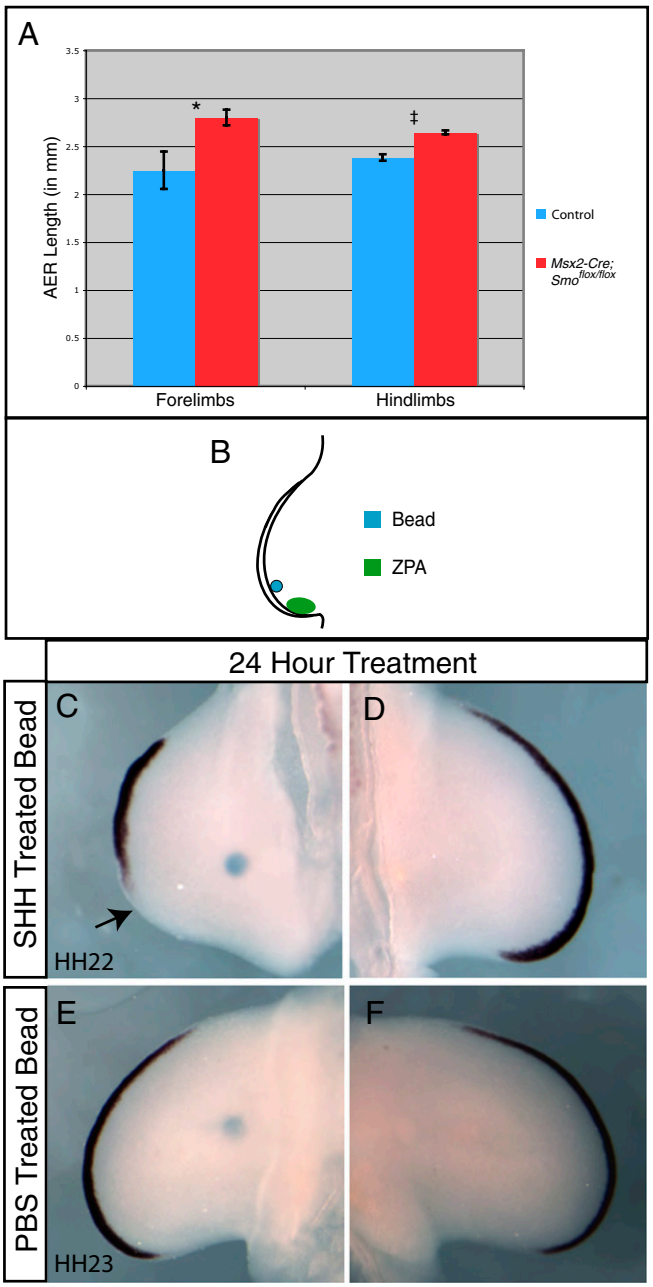

Fig. 3. Removal of hedgehog signaling in the AER results in an increase in AER length. (*A*) Average AER length after measurement of *Fgf8* expression in *Msx2-Cre;Smo*$^{flox/flox}$ limbs and control limbs using the Straighten plug-in for NIH ImageJ. Data are represented as means and the error bars represent the SEM. A *t* test (Welch's; unpaired) indicated that these differences were statistically significant (*, $P = 0.03$; ‡, $P < 0.0001$). (*B*) A diagram of chick limbs with a bead soaked in SHH implanted just anterior to the ZPA in the distal limb bud mesenchyme. *Fgf8* expression was decreased after 24 h of treatment with a SHH soaked bead beginning at HH 20 (*C*) compared to an untreated contralateral control limb (*D*). The arrow in *C* highlights the loss of posterior AER in the treated limb bud. *Fgf8* expression after 24 h of treatment with a PBS soaked bead was unchanged (*E*) when compared with a contralateral control limb (*F*) The proximal location of the beads in (*C* and *E*) 24 h after implantation is a result of outgrowth of the limb bud.

was more broad when compared with somite matched control limbs (Fig. 4 *E* and *F*). These data indicate that proper regulation of the *Shh*/*Grem1*/*Fgf* feedback loop requires activation of the Hh signaling pathway in the limb bud AER.

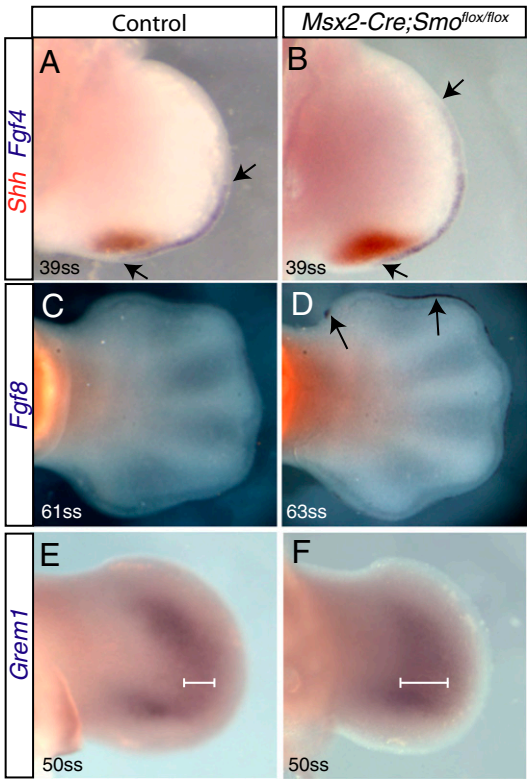

Fig. 4. Gene expression in *Msx2-Cre;Smo*$^{flox/flox}$ limbs. (*A* and *B*) Double-labeled RNA in situ hybridizations of control and *Msx2-Cre;Smo*$^{flox/flox}$ hindlimbs for *Shh* (red) and *Fgf4* (purple) revealed an increase in *Fgf4* and *Shh* expression at 39ss. Arrows mark the anterior and posterior limit of *Fgf4* expression. (*C* and *D*) Comparison of *Fgf8* expression in 61ss (control) and 63ss (*Msx2-Cre;Smo*$^{flox/flox}$) hindlimbs revealed that *Fgf8* expression was prolonged in *Msx2-Cre;Smo*$^{flox/flox}$ compared with control limbs. Arrows in *D* denote prolonged expression of *Fgf8*. Expression of *Grem1* was expanded at 50ss in *Msx2-Cre;Smo*$^{flox/flox}$ compared with wild-type hindlimbs (*E* and *F*). White lines in *E* and *F* show the width of the domain of *Grem1* expression.

Discussion

Within the vertebrate limb mesoderm, several different roles for SHH have been reported. SHH acts through a concentration gradient (1) and a temporal gradient (3) to establish both digit identity and number. Additionally, through regulation of genes that promote the G_1-S transition, SHH affects limb patterning by controlling growth (4, 5). In this study, we present evidence that Hh signaling is present in the AER and is required within the AER for correct patterning of the vertebrate autopod.

Activation of the Hh signaling pathway was detected in several domains within the posterior ectoderm of the developing limb. Because *Shh* expression in the limb bud ectoderm has not been detected by RNA in situ hybridization (27) or microarrays (26), Hh signals to the ectoderm through a paracrine mechanism.

Targets of the Hh signaling pathway were found in the AER, the dorsal and ventral ectoderm, and the ectoderm of the posterior margin (ectoderm between the AER and the flank). After removal of Hh signaling from the AER, Hh signaling remained in ectodermal cells juxtaposed to the posterior AER. The lack of a stronger phenotype upon removal of Hh signaling from the AER may be due to the presence of Hh-responding cells in the posterior margin. Active hedgehog signaling in this region of the limb bud may be able to compensate for a loss of Hh signaling in the AER by specifying the posterior limit of the AER. Removal of Hh signaling from both the AER and the posterior margin has

the potential to result in a more significant expansion of the AER and an increase in the severity of polydactyly.

Upon removal of Hh signaling from the AER, we observed changes in gene expression of components of the *Shh*/*Grem1*/*Fgf* feedback loop. Removal of Hh signaling from the AER increased the length of the AER, resulting in an increase in the number of cells capable of expressing *Fgf4* and *Fgf8*. Previous experiments have shown that *Fgf4* expressed from the AER can regulate *Shh* expression in the ZPA (41, 43), suggesting that the increase in *Shh* expression we observed is a result of an increase in the amount of FGF4 produced in the AER.

Previously, *Grem1* expression has been shown to be regulated by the Hh signaling pathway in the limb bud mesenchyme (12, 44). Our data suggests that increased *Fgf4* from the AER indirectly increases expression of *Grem1* through activation of *Shh* in limb buds that have Hh signaling removed from the AER. During normal limb development, *Grem1* is required for *Fgf8* expression from the AER (15, 45). The observed increase in *Grem1* expression upon loss of Hh signaling from the AER may explain the perdurance of *Fgf8* expression in the limb bud AER.

Although perdurance of components of the *Shh*/*Grem1*/*Fgf* feedback loop was observed in limbs lacking Hh signaling within the AER, formation of extra cartilaginous condensations did not occur until after expression of genes known to be involved in the *Shh*/*Grem1*/*Fgf* feedback loop had terminated. The extra cartilaginous condensations could be a result of an increase in mesodermal cell number caused by early changes in gene expression.

The amount of SHH produced in the limb bud has been shown to control the number of *Shh*-expressing cells in the ZPA through cell death (6). Consistent with the observations of Sanz-Ezquerro and Tickle (6), our experiments increasing SHH in the posterior of the chick limb induced cell death. In addition to an increase in cell death, we identified a reduction in AER length detected by *Fgf4* and *Fgf8* expression after elevating SHH protein levels in the limb bud mesenchyme. Our experiments, in which we either genetically removed Hh signaling from the AER or ectopically elevated SHH protein in the limb mesenchyme, indicate that Hh signaling in the AER refines the length of the AER resulting in potential changes in the number of cells expressing *Fgf4* and *Fgf8*.

We propose that changes to the AER in response to the Hh signaling pathway during normal limb development refine the initial levels of SHH produced by the ZPA through changes induced by *Fgf* expression. During normal limb development, the initial levels of SHH produced by the ZPA are likely to vary between embryos and possibly even within the limbs buds of a given embryo. To ensure normal patterning, the pool of *Shh*-expressing cells has to be refined to produce an exact and reproducible amount of SHH in every limb bud. We propose that during normal development, if the original pool of cells in the ZPA produces too much SHH, there is a corresponding increase in Hh signaling in the AER, resulting in a decrease in AER length. SHH-producing cells are then removed from the ZPA (6). If too little SHH is produced, Hh signaling in the AER decreases, resulting in an increase in AER length and a corresponding increase in SHH production in the ZPA (see model in Fig. 5). In our model, the ability of the AER to directly respond to SHH facilitates the production of a reproducible concentration of SHH in every limb bud within a given species. In normal limbs, the proposed changes in the length of the AER and SHH produced from the ZPA are most likely very subtle because large alterations in either SHH protein or AER length would result in defects in autopod patterning.

Regulation of *Shh* expression in the mesoderm of appendages including fins has been identified as a potential source of morphological change over the course of evolution (46). We propose that the response to Hh signaling within the ectoderm could also function as a source of evolutionary change. Because Hh signaling in the ectoderm is required for patterning the autopod, it is possible that by changing the ability of limb bud ectodermal cells to respond to SHH, digit number could be altered during evolution.

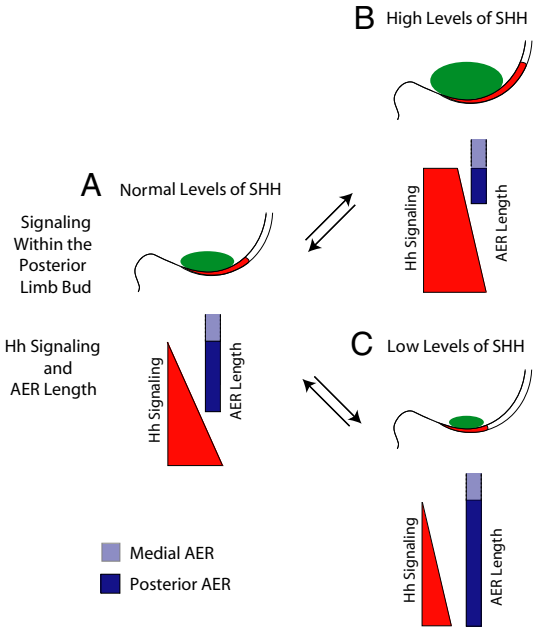

Fig. 5. Model of stochastic control of AER length by hedgehog signal transduction within the AER. During normal development, a population of cells within the ZPA expresses *Shh*. Response to Hh signaling within the ectoderm limits or expands the length of the AER. If levels of SHH protein in the AER are elevated (*B*), the AER is shortened because of elevated Hh signaling in this tissue. Shortening of the AER results in a corresponding decrease in mesenchymal *Shh* expression. If levels of SHH protein are decreased or absent from the AER (*C*), decreased Hh signaling occurs in the AER and the AER expands in length. As a result of a longer AER, there is a corresponding increase in *Shh* expression in the underlying mesenchyme. This buffering mechanism ensures that the amount of SHH produced from the ZPA is appropriate and results in a reproducible digit pattern (*A*). In the model, only the posterior of the limb bud is diagramed. Green in the mesenchyme shows the level of *Shh* expression in the ZPA, whereas red in the AER denotes Hh signaling. Dark blue denotes the posterior AER where we identified targets of Hh signaling. The more anterior AER is shown as light blue.

Methods

Mouse Alleles and Breeding. The *Shh*$^{\Delta}$, *Gli1-CreER*^{T2}, *R26R*, *Ptch1:LacZ*, *Msx2-Cre*, and *Smo*^{flox} alleles were maintained and genotyped as described (2, 31, 34, 35, 42, 47). Genotyping was performed on DNA isolated from tail or yolk sack tissue. Embryos harvested at E12.5 or earlier were staged by counting somites. For experiments involving embryos lacking *Smo* in the AER, control embryos lacked the *Msx2-Cre* allele and were either heterozygous or homozygous for the *Smo*^{flox} allele. Both genetic combinations were phenotypically indistinguishable from normal mice. Alleles were maintained on mixed backgrounds, and animals were handled in accordance with the University of Florida Institutional Animal Care and Use Committee.

Fate Mapping, β-Galactosidase Detection, and Immunohistochemistry. Tamoxifen was administered in corn oil (Sigma; C-8267) at a final concentration of 20 mg/mL by oral gavage as described (2). For whole-mount detection of β-galactosidase activity, embryos were harvested and fixed overnight in 0.2% formaldehyde. After fixation, β-galactosidase activity was detected as described (3). For β-galactosidase detection on sections, embryos were fixed and cryoprotected with 30% sucrose in PBS. After embedding in O.C.T. compound (Sakura; 4583), cryoprotected embryos were sectioned at 12 microns. Slide-mounted tissue was washed two times with PBS before being incubated overnight at 37 °C in staining solution [1 mg/mL X-Gal, 5 mM $K_3Fe(CN)_6$ and 5 mM $K_4Fe(CN)_6$ in concentrated rinse buffer (0.1 M NaH_2PO_4 at pH 7.4, 2 mM $MgCl_2$, 0.2% Igepal, 0.1% sodium deoxycholate)]. Stained tissue was rinsed three times with PBS, dehydrated, and mounted with Permount (Fisher SP15-500). SHH immunohistochemistry was performed as described (28).

DEVELOPMENTAL BIOLOGY

Whole-Mount RNA in Situ Hybridization and AER Measurement. Embryos harvested for in situ hybridization were incubated overnight in 4% formaldehyde at 4 °C. Section and whole-mount RNA in situ hybridizations were performed according to a standard protocol (48) with the exception that BM Purple (Roche; 1442074) was used in place of NBT and BCIP to develop *Ptch1 in situs*. *Smo* riboprobe (used in Fig. S3) synthesis was performed on a plasmid constructed by RT-PCR using the following primers: forward, 5′-ttcccagggttgaagacag, reverse, 5′-cacgttgtagcgcaaag. AER length was calculated by importing pictures into NIH ImageJ (49). A calibration plate was measured at the same magnification to set the scale. The "Straighten" plug-in was used to turn the curved AERs into measurable straight lines (50). The mean AER length of *Msx2-Cre;Smo*$^{flox/flox}$ forelimbs (50ss; $n = 9$) and hindlimbs (50ss; $n = 10$), and control forelimbs (50ss; $n = 4$) and hindlimbs (50ss; $n = 7$) was collected, and a *t* test (Welch's; unpaired) was used to test the significance ($\alpha = 0.05$).

Bead Implantation and LysoTracker Analysis. Affi-gel beads (Bio Rad, 153–7302) were soaked in hrSHH (1 mg/mL in PBS; R&D Systems; 1845-SH) or PBS for at least one hour. Chicks were staged according to the staging guide by Hamburger and Hamilton (51). Eggs were fenestrated with laminectomy forceps. At HH stage 20, the amnionic raphe was separated and a bead was transferred to the egg by using watchmakers forceps. Next, a microdissection needle was used to create a small hole in the mesenchyme proximal to the AER in a region just anterior to the ZPA. The bead was inserted into the space created by the microdissecting needle, and the embryos were placed at 37 °C overnight. Embryos were harvested after 24 h of incubation and fixed in 4% formaldehyde at 4 °C overnight before further analysis. Lysotracker (Molecular Probes; L-7528), an acidophilic dye that accumulates in the lysosmes of apoptotic cells and phagocytic cells engulfing apoptotic cells (52), was used as previously described (53).

ACKNOWLEDGMENTS. We thank W. J. Scott, M. McFarlane, S. A. Vokes, and A. P. McMahon for helpful discussion, sharing unpublished data, and for commenting on an early draft of this work. Some probes used in this report were generous gifts from C. J. Tabin (Harvard Medical School) and M. J. Cohn (University of Florida). A.G.-L. is supported by the Swedish Research Council-Medicine Grants 1581 and 20614 and the Institute of Odontology, Sahlgrenska Academy. This work was supported by start-up funds granted to B. D.H. from the University of Florida, College of Medicine.

1. Yang Y, et al. (1997) Relationship between dose, distance and time in Sonic Hedgehog-mediated regulation of anteroposterior polarity in the chick limb. *Development* 124:4393–4404.
2. Ahn S, Joyner AL (2004) Dynamic changes in the response of cells to positive hedgehog signaling during mouse limb patterning. *Cell* 118:505–516.
3. Harfe BD, et al. (2004) Evidence for an expansion-based temporal Shh gradient in specifying vertebrate digit identities. *Cell* 118:517–528.
4. Towers M, Mahood R, Yin Y, Tickle C (2008) Integration of growth and specification in chick wing digit-patterning. *Nature* 452:882–886.
5. Zhu J, et al. (2008) Uncoupling Sonic hedgehog control of pattern and expansion of the developing limb bud. *Dev Cell* 14:624–632.
6. Sanz-Ezquerro JJ, Tickle C (2000) Autoregulation of Shh expression and Shh induction of cell death suggest a mechanism for modulating polarising activity during chick limb development. *Development* 127:4811–4823.
7. Goetz JA, Suber LM, Zeng X, Robbins DJ (2002) Sonic Hedgehog as a mediator of long-range signaling. *Bioessays* 24:157–165.
8. Fuse N, et al. (1999) Sonic hedgehog protein signals not as a hydrolytic enzyme but as an apparent ligand for patched. *Proc Natl Acad Sci USA* 96:10992–10999.
9. Murone M, Rosenthal A, de Sauvage FJ (1999) Sonic hedgehog signaling by the patched-smoothened receptor complex. *Curr Biol* 9:76–84.
10. Hooper JE, Scott MP (2005) Communicating with Hedgehogs. *Nat Rev Mol Cell Biol* 6:306–317.
11. Vokes SA, et al. (2007) Genomic characterization of Gli-activator targets in sonic hedgehog-mediated neural patterning. *Development* 134:1977–1989.
12. Vokes SA, Ji H, Wong WH, McMahon AP (2008) A genome-scale analysis of the cis-regulatory circuitry underlying sonic hedgehog-mediated patterning of the mammalian limb. *Genes Dev* 22:2651–2663.
13. Laufer E, Nelson CE, Johnson RL, Morgan BA, Tabin C (1994) Sonic hedgehog and Fgf-4 act through a signaling cascade and feedback loop to integrate growth and patterning of the developing limb bud. *Cell* 79:993–1003.
14. Yang Y, Niswander L (1995) Interaction between the signaling molecules WNT7a and SHH during vertebrate limb development: Dorsal signals regulate anteroposterior patterning. *Cell* 80:939–947.
15. Khokha MK, Hsu D, Brunet LJ, Dionne MS, Harland RM (2003) Gremlin is the BMP antagonist required for maintenance of Shh and Fgf signals during limb patterning. *Nat Genet* 34:303–307.
16. Panman L, et al. (2006) Differential regulation of gene expression in the digit forming area of the mouse limb bud by SHH and gremlin 1/FGF-mediated epithelial-mesenchymal signalling. *Development* 133:3419–3428.
17. Bénazet JD, et al. (2009) A self-regulatory system of interlinked signaling feedback loops controls mouse limb patterning. *Science* 323:1050–1053.
18. Scherz PJ, Harfe BD, McMahon AP, Tabin CJ (2004) The limb bud Shh-Fgf feedback loop is terminated by expansion of former ZPA cells. *Science* 305:396–399.
19. Verheyden JM, Sun X (2008) An Fgf/Gremlin inhibitory feedback loop triggers termination of limb bud outgrowth. *Nature* 454:638–641.
20. Mao J, McGlinn E, Huang P, Tabin CJ, McMahon AP (2009) Fgf-dependent Etv4/5 activity is required for posterior restriction of Sonic Hedgehog and promoting outgrowth of the vertebrate limb. *Dev Cell* 16:600–606.
21. Zhang Z, Verheyden JM, Hassell JA, Sun X (2009) FGF-regulated Etv genes are essential for repressing Shh expression in mouse limb buds. *Dev Cell* 16:607–613.
22. Niswander L (2002) Interplay between the molecular signals that control vertebrate limb development. *Int J Dev Biol* 46:877–881.
23. Pearse RV, 2nd, Vogan KJ, Tabin CJ (2001) Ptc1 and Ptc2 transcripts provide distinct readouts of Hedgehog signaling activity during chick embryogenesis. *Dev Biol* 239:15–29.
24. Quirk J, et al. (1997) The smoothened gene and hedgehog signal transduction in Drosophila and vertebrate development. *Cold Spring Harb Symp Quant Biol* 62:217–226.
25. Bell SM, Schreiner CM, Scott WJ (1999) Disrupting the establishment of polarizing activity by teratogen exposure. *Mech Dev* 88:147–157.
26. Bell SM, Schreiner CM, Goetz JA, Robbins DJ, Scott WJ, Jr (2005) Shh signaling in limb bud ectoderm: potential role in teratogen-induced postaxial ectrodactyly. *Dev Dyn* 233:313–325.
27. Riddle RD, Johnson RL, Laufer E, Tabin C (1993) Sonic hedgehog mediates the polarizing activity of the ZPA. *Cell* 75:1401–1416.
28. Gritli-Linde A, Lewis P, McMahon AP, Linde A (2001) The whereabouts of a morphogen: direct evidence for short- and graded long-range activity of hedgehog signaling peptides. *Dev Biol* 236:364–386.
29. Bitgood MJ, McMahon AP (1995) Hedgehog and Bmp genes are coexpressed at many diverse sites of cell-cell interaction in the mouse embryo. *Dev Biol* 172:126–138.
30. Marigo V, Johnson RL, Vortkamp A, Tabin CJ (1996) Sonic hedgehog differentially regulates expression of GLI and GLI3 during limb development. *Dev Biol* 180:273–283.
31. Soriano P (1999) Generalized lacZ expression with the ROSA26 Cre reporter strain. *Nat Genet* 21:70–71.
32. St-Jacques B, Hammerschmidt M, McMahon AP (1999) Indian hedgehog signaling regulates proliferation and differentiation of chondrocytes and is essential for bone formation. *Genes Dev* 13:2072–2086.
33. Marigo V, Scott MP, Johnson RL, Goodrich LV, Tabin CJ (1996) Conservation in hedgehog signaling: induction of a chicken patched homolog by Sonic hedgehog in the developing limb. *Development* 122:1225–1233.
34. Goodrich LV, Milenković L, Higgins KM, Scott MP (1997) Altered neural cell fates and medulloblastoma in mouse patched mutants. *Science* 277:1109–1113.
35. Zhang XM, Ramalho-Santos M, McMahon AP (2001) Smoothened mutants reveal redundant roles for Shh and Ihh signaling including regulation of L/R asymmetry by the mouse node. *Cell* 105:781–792.
36. Barrow JR, et al. (2003) Ectodermal Wnt3/beta-catenin signaling is required for the establishment and maintenance of the apical ectodermal ridge. *Genes Dev* 17:394–409.
37. Lee J, Tickle C (1985) Retinoic acid and pattern formation in the developing chick wing: SEM and quantitative studies of early effects on the apical ectodermal ridge and bud outgrowth. *J Embryol Exp Morphol* 90:139–169.
38. Todt WL, Fallon JF (1984) Development of the apical ectodermal ridge in the chick wing bud. *J Embryol Exp Morphol* 80:21–41.
39. Crossley PH, Martin GR (1995) The mouse Fgf8 gene encodes a family of polypeptides and is expressed in regions that direct outgrowth and patterning in the developing embryo. *Development* 121:439–451.
40. Mahmood R, et al. (1995) A role for FGF-8 in the initiation and maintenance of vertebrate limb bud outgrowth. *Curr Biol* 5:797–806.
41. Lewandoski M, Sun X, Martin GR (2000) Fgf8 signalling from the AER is essential for normal limb development. *Nat Genet* 26:460–463.
42. Sun X, et al. (2000) Conditional inactivation of Fgf4 reveals complexity of signalling during limb bud development. *Nat Genet* 25:83–86.
43. Lu P, Minowada G, Martin GR (2006) Increasing Fgf4 expression in the mouse limb bud causes polysyndactyly and rescues the skeletal defects that result from loss of Fgf8 function. *Development* 133:33–42.
44. Nissim S, Hasso SM, Fallon JF, Tabin CJ (2006) Regulation of Gremlin expression in the posterior limb bud. *Dev Biol* 299:12–21.
45. Michos O, et al. (2004) Gremlin-mediated BMP antagonism induces the epithelial-mesenchymal feedback signaling controlling metanephric kidney and limb organogenesis. *Development* 131:3401–3410.
46. Dahn RD, Davis MC, Pappano WN, Shubin NH (2007) Sonic hedgehog function in chondrichthyan fins and the evolution of appendage patterning. *Nature* 445:311–314.
47. Chiang C, et al. (1996) Cyclopia and defective axial patterning in mice lacking Sonic hedgehog gene function. *Nature* 383:407–413.
48. Wilkinson DG, Nieto MA (1993) Detection of messenger RNA by in situ hybridization to tissue sections and whole mounts. *Methods Enzymol* 225:361–373.
49. Rasband WS, (1997–2007) Image J U.S National Institute of Health, Bethesda, MD, http://rsb.info.nih.gov/ij/.
50. Kocsis E, Trus BL, Steer CJ, Bisher ME, Steven AC (1991) Image averaging of flexible fibrous macromolecules: The clathrin triskelion has an elastic proximal segment. *J Struct Biol* 107:6–14.
51. Hamburger V, Hamilton HL (1951) A series of normal stages in the development of the chick embryo. *J Morphol* 88:49–92.
52. Zucker RM, Hunter ES, 3rd, Rogers JM (1999) Apoptosis and morphology in mouse embryos by confocal laser scanning microscopy. *Methods* 18:473–480.
53. Bouldin CM, Harfe BD (2009) Aberrant FGF signaling, independent of ectopic hedgehog signaling, initiates preaxial polydactyly in Dorking chickens. *Dev Biol* 334:133–141.